AEM
Journals.ASM.org

Identification and Characterization of the *Rhizobium* sp. Strain GIN611 Glycoside Oxidoreductase Resulting in the Deglycosylation of Ginsenosides

Eun-Mi Kim,[a] Juhan Kim,[b] Joo-Hyun Seo,[a] Jun-Seong Park,[c] Duck-Hee Kim,[c] and Byung-Gee Kim[a]

School of Chemical and Biological Engineering, Seoul National University, Seoul, Republic of Korea[a]; Cooperative Institute for Research in Environmental Sciences, University of Colorado, Boulder, Colorado, USA[b]; and R & D Center, Amore-Pacific Corporation, Yong-In, Kyounggi-do, Republic of Korea[c]

Using enrichment culture, *Rhizobium* sp. strain GIN611 was isolated as having activity for deglycosylation of a ginsenoside, compound K (CK). The purified heterodimeric protein complex from *Rhizobium* sp. GIN611 consisted of two subunits with molecular masses of 63.5 kDa and 17.5 kDa. In the genome, the coding sequence for the small subunit was located right after the sequence for the large subunit, with one nucleotide overlapping. The large subunit showed CK oxidation activity, and the deglycosylation of compound K was performed via oxidation of ginsenoside glucose by glycoside oxidoreductase. Coexpression of the small subunit helped soluble expression of the large subunit in recombinant *Escherichia coli*. The purified large subunit also showed oxidation activity against other ginsenoside compounds, such as Rb1, Rb2, Rb3, Rc, F2, CK, Rh2, Re, F1, and the isoflavone daidzin, but at a much lower rate. When oxidized CK was extracted and incubated in phosphate buffer with or without enzyme, (*S*)-protopanaxadiol [PPD(S)] was detected in both cases, which suggests that deglycosylation of oxidized glucose is spontaneous.

Ginseng is a traditional plant medicine that has been widely used for preventive and therapeutic purposes in Asian countries over thousands of years. It exhibits various pharmacological effects, such as anticancer, anti-inflammation, and antiaging effects (3, 6, 26, 35). The main physiologically active compounds of ginseng are ginsenosides, which have over 40 kinds of known structures that generally fall into three different classes: the protopanaxadiol (PPD), protopanaxatriol (PPT), and oleanolic acid types (14, 31). Previous studies reported that the pharmacological functions of ginsenosides come from the deglycosylated forms of ginsenosides generated by intestinal bacteria (3, 14, 29, 32, 34). The absorption of ginsenosides in the human intestine is greatly affected by the presence of glycosyl moieties in their structures. In general, glycosylated ginsenoside is poorly absorbed into the bloodstream compared to the deglycosylated form due to its hydrophilicity. Therefore, the deglycosylated forms often show better pharmacological activity in the body than the glycosylated forms (17, 21). For example, the ginsenosides compound K (CK) and Rh2, which are widely known as inducers of tumor cell apoptosis (10, 18), are deglycosylated into PPD. Compared to Rh2, PPD shows better pharmacological effects on B16 melanoma cells (28). Deglycosylation of ginsenosides in the human body varies greatly depending upon the enzyme activity of microbial flora in the intestines. Since this activity varies between individuals, the medicinal effects of ginseng also vary significantly (39). To understand the exact pharmacological effects of the deglycosylated ginsenosides, a pure compound of deglycosylated ginsenoside should be used or administered. However, since it is difficult to obtain a large quantity of such rare deglycosylated ginsenosides, their biological roles and pharmacological effects (6) have not been thoroughly studied.

Recent research on ginsenosides is focused mainly on the production of rare and effective ginsenosides through enzymatic deglycosylation (13, 19, 22, 23, 38). There have been several attempts to produce such biologically active deglycosylated ginsenosides (2, 15, 16, 29), using microbial transformation (7, 8), enzymatic deglycosylation (23, 33), and mild acid hydrolysis (12). Among them, enzymatic deglycosylation is the most preferred method, since it is substrate specific, produces fewer by-products, requires simple separation, results in high yields, and is environmentally friendly. Thus far, the isolation of various intestinal anaerobic and food bacteria (e.g., *Fusobacterium* strain K-60, *Bifidobacterium* sp. strain SJ32, and *Lactobacillus delbrueckii*) (5, 9, 29) and soil bacteria from ginseng farms (e.g., *Fusarium sacchari*) (13, 41) has been reported. In addition, various glycoside-hydrolyzing enzymes (e.g., β-glucosidase having deglycosylation activity on Rg3) (1, 5, 37, 40, 41) from such microorganisms were isolated for ginsenoside production.

Although there are some reports already available on glycosidases that produce CK (13, 37, 40) from various major ginsenosides, there are no reports on enzymatic deglycosylation of CK to produce (*S*)-PPD [PPD(S)]. Some microorganisms (e.g., *Eubacterium* strain A44 and *Bacteroides* strain HJ15) (2) have been reported as having deglycosylation activities converting CK or Rh2 into PPD(S), but with very low productivity. To produce a large amount of rare deglycosylated ginsenosides using enzymes, microorganisms showing serial and/or stepwise deglycosylation activity emulating that of intestinal bacteria flora in the human body are required. This study focuses on the screening of novel microorganisms that have deglycosylation activity for CK (Fig. 1) and

Received 2 August 2011 **Accepted** 14 October 2011
Published ahead of print 21 October 2011
Address correspondence to Byung-Gee Kim, byungkim@snu.ac.kr.
Supplemental material for this article may be found at http://aem.asm.org/.

doi:10.1128/AEM.06404-11

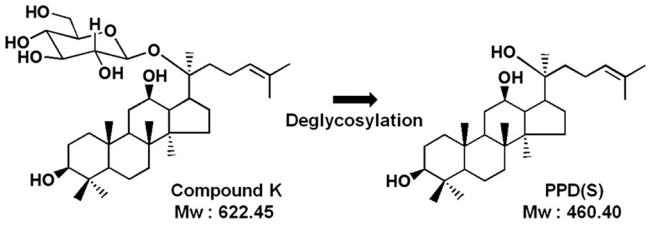

FIG 1 Target reaction scheme for the ginsenoside compound K (CK).

the isolation of deglycosylating enzymes from the screened microorganism.

MATERIALS AND METHODS

Chemicals. Red ginseng extract, a mixture of various ginsenosides, was prepared by ethyl acetate extraction, and CK (50%) was produced by enzymatic biotransformation by the method of Kim et al. (20). Other ginsenosides, i.e., Rb2, Rb3, Rc, Rd, F2, Rh2, PPD(S), Re, and F1, were purchased from LKT Laboratories Inc. (St. Paul, MN), and ginsenoside Rb1 was purchased from Wako Pure Chemical Co., Ltd. (Osaka, Japan). The isoflavone daidzin was purchased from Sigma (St. Louis, MO) (see Table S2 in the supplemental material). All solvents for high-pressure liquid chromatography (HPLC) analysis were of HPLC grade and from Duksan Pure Chemical (Ansan, Republic of Korea). Methanol and ethanol were purchased from Merck Chemical (Darmstadt, Germany). Chloroform was purchased from Junsei Chemical (Tokyo, Japan). The chemicals required for protein assay and sodium dodecyl sulfate-polyacrylamide gel electrophoresis (SDS-PAGE) were purchased from Bio-Rad (Hercules, CA). All other chemicals were purchased from Sigma (St. Louis, MO).

Screening of microorganisms. An enrichment culture was performed to isolate a new microorganism which had the ability to catalyze the deglycosylation of the ginsenoside CK. After field soil samples from a ginseng farm (10 g) were mixed with 50 ml phosphate-buffered saline (PBS), the mixture was filtered using filter paper (alpha cotton cellulose, 110-mm diameter; Advantec, Japan). The filtered sample (100 μl) was inoculated into 10 ml minimal M9-ginsenoside medium with a 0.2% (wt/vol) red ginseng extract (ginsenoside mixture) as a carbon source instead of glucose. Cultures were grown at 30°C under aerobic conditions. After several rounds of enrichment cultures, the culture media were diluted, spread on an M9-ginsenoside minimal medium or Luria-Bertani medium (LB) agar plate, and incubated at 30°C for 20 h. Fifty colonies were selected randomly, based on differences in morphology and color. The selected cells were subsequently cultured in 3 ml of M9-ginsenoside medium at 30°C. Cultured cells were stored at −80°C for further study. After the cells were harvested and washed using PBS, whole-cell reactions were performed to find strains with CK deglycosylation activity. Strains with high CK deglycosylation activity were selected. 16S rRNA sequencing (SolGent Co., Daejeon, Republic of Korea) was performed to identify the screened microorganism.

Enzyme assay and analytical methods. For screening of microorganisms showing ginsenoside deglycosylation activity, matrix-assisted laser desorption ionization–time of flight (MALDI-TOF) mass spectrometry (MS) (Biflex IV; Bruker Daltonics, Bremen, Germany) was used. For whole-cell reactions, a cell pellet was obtained by centrifugation from 3 ml M9-ginsenoside medium after growth at 30°C for 12 h. The pellets were resuspended in 1 ml of 50 mM sodium phosphate buffer (pH 7.0) containing 50 μM CK. The mixture was incubated at 37°C for 12 h. Reactants and products were extracted with 1 ml ethyl acetate. The extracted samples went through evaporation using a vacuum concentrator (Biotron, Seoul, Republic of Korea). The dried reaction samples were dissolved in ethanol and then analyzed by MALDI-TOF using 2,5-dihydroxybenzoic acid as a matrix.

For confirmation of the activity of the active fraction during the protein purification, thin-layer chromatography (TLC) analysis was performed with silica gel 60 F_{254} plates (Merck, Darmstadt, Germany). Separation was with $CHCl_3$-methanol-H_2O (65:35:10, vol/vol/vol), and visualization was with 10% H_2SO_4 in ethanol and application of heat.

Quantitative analysis of the CK deglycosylation reaction was performed using a high-pressure liquid chromatography (HPLC) system (Younglin Instrument, Seoul, Republic of Korea) equipped with a Symmetry C_{18} 5-μm column (4.6 by 150 mm; Waters, MA). The HPLC analysis was performed using an 80% acetonitrile (ACN) aqueous solution as an eluent with a flow rate of 0.8 ml/min and a detection wavelength of 203 nm. Reaction profiles of F2 were analyzed with HPLC using gradient elution at a flow rate of 1 ml/min, consisting of the following steps: 30% ACN–70% H_2O for 5 min, a gradual increase to 80% ACN–20% H_2O for 35 min, further retention for 15 min, 100% ACN for an additional 10 min, a decrease to 30% ACN–70% H_2O for 2 min, and 30% ACN–70% H_2O for 10 min.

Purification of the active protein. For the purification of the deglycosylation enzyme, the screened microorganism was cultured in 10 liters of M9-ginsenoside medium. The cells were harvested by centrifugation at 3,000 × *g* for 15 min and washed with PBS. The pellet was resuspended in 50 mM sodium phosphate buffer (pH 7.0) containing 1 mM EDTA, 1 mM phenylmethylsulfonyl fluoride (PMSF), and 1 mM dithiothreitol (DTT). To obtain the cell extract, the cells were disrupted by sonication and debris was removed by centrifugation at 20,000 × *g* for 40 min. All purification steps were carried out at 4°C, and proteins in each fraction were monitored using SDS-PAGE. Column chromatography for protein purification was performed with an ÄKTA system (GE Healthcare Europe GmbH, Germany). The extract was fractionated by ammonium sulfate precipitation (between 60 and 70% saturation). The prepared sample was loaded on a Q-Sepharose FF column (1.6 by 10 cm; GE Healthcare, NJ) preequilibrated with 20 mM Tris-HCl (pH 7.4) and was eluted with 20 mM Tris-HCl (pH 7.4) by a linear gradient of KCl from 0 to 0.5 M. The active fractions were collected, concentrated with Amicon Ultra-15 centrifugal filter units (molecular weight cutoff [MWCO], 10,000; Millipore Corporation, Bedford, MA), and applied to a Sephacryl S-200 column (1.6 by 60 cm; GE Healthcare) preequilibrated with 50 mM sodium phosphate buffer (pH 7.5) containing 0.15 M sodium chloride. The separated active fraction was loaded on a HiTrap phenyl HP column (1-ml column volume; GE Healthcare) preequilibrated with 50 mM sodium phosphate buffer (pH 7.5) containing 1 M ammonium sulfate. The proteins were eluted using a linear gradient of ammonium sulfate from 1 M to 0 M in 50 mM sodium phosphate buffer (pH 7.5) at a flow rate of 1 ml/min. The active fractions were pooled and concentrated with an Amicon Ultra-4 centrifugal filter unit (MWCO, 10,000; Millipore Corporation). The obtained active fraction was applied to a Superdex S-200 column (1.0 by 30 cm; GE Healthcare) preequilibrated with 50 mM sodium phosphate buffer (pH 7.5) containing 0.15 M sodium chloride. The final active fraction was separated by native gel (4 to 16% NativePAGE Novex Bis-Tris; Invitrogen Korea, Seoul, Republic of Korea) electrophoresis. In the analysis of the native gel electrophoresis, anode buffer (NativePAGE running buffer; Invitrogen Korea) and cathode buffer (NativePAGE running buffer and NativePAGE cathode additive; Invitrogen Korea) were used. The NativePAGE cathode additive contained 0.002% Coomassie blue G-250. After the native gel was stained with cathode buffer, the stained bands were sliced and the sliced gels were reacted to select the active protein band. The active band was sliced and crushed into small pieces, which were used to load samples for SDS-PAGE (12%).

Analysis of peptide sequences from isolated proteins. To determine the N-terminal amino acid sequence, a protein band from 12% SDS-PAGE was transferred to a polyvinylidene fluoride (PVDF) membrane. As two bands (see Fig. S2 in the supplemental material) appeared on SDS-PAGE with the final sample of the purified enzyme, both bands were used for N-terminal sequencing using automated Edman degradation with a Procise 492 cLC protein sequencer (Applied Biosystems, Foster City, CA) at the Korea Basic Science Institute (Seoul, Republic of Korea). For inter-

nal peptide sequencing, the previous two protein bands were isolated from the SDS-PAGE and digested with sequencing-grade trypsin (Promega, Madison, WI) to obtain tryptic fragments for mass analysis. The peptide sequences of tryptic fragments were determined with an LTQ-Orbitrap (Thermo Electron Corp., San Jose, CA) with a nanospray source in the positive-ion mode. The spray tip for the nanospray was made using the method of Gatlin et al. (11) with a P-2000 laser puller (Shutter Instrument, Novato, CA). The trypsin-digested sample was loaded onto a capillary spray tip packed with XDB-C_{18} resin with a diameter of 5 μm (Agilent, Palo Alto, CA) using a high-pressure chamber under 1 MPa of nitrogen gas. The loaded sample was eluted using a 5 to 100% linear gradient with ACN at a flow rate of 0.3 μl/min. The obtained mass spectrum was analyzed using a *de novo* sequencing program, PEAKS 4.5 (Bioinformatics Solutions Inc., Waterloo, Canada).

Analysis of structural genes. Degenerate primers were designed based on the N-terminal sequence and the internal peptide sequences shown in Table S1 in the supplemental material. The genomic DNA of the screened microorganism was prepared using a G-spin genomic DNA extraction kit (iNtRON, Seongnam-si, Gyeonggi-do, Republic of Korea). The first PCR was performed with the degenerate primers and genomic DNA of the screened microorganism using *Taq* polymerase (Cosmo Co. Ltd., Seoul, Republic of Korea). The obtained PCR products were cloned in pGEM-T vector (Promega, Madison, WI) for analysis of the gene sequence. From the sequencing results, partial sequences of a structural gene were obtained. To obtain the entire structural gene sequence, the inverse PCR method was used. The genomic DNA was digested with HindIII restriction enzyme (Koschem, Seoul, Republic of Korea), and fragments were self-ligated using T4 DNA ligase (New England BioLabs, Ipswich, MA). The HindIII cleavage site is located in the C terminus (bp 1294 to 1299) of the obtained partial sequence. Inverse PCR was performed in the outward direction on the obtained partial sequence of the structural gene using the cyclized genomic DNA library and two primers (forward primer 5′-CTG CATGACGTCTGCTGCCTGTGTA-3′, bp 1581 to 1605; reverse primer 5′-CACCATGTCTTCACGCATATCGAGT-3′, bp 1368 to 1392) which bound to the C-terminal region of the obtained partial sequence (see Fig. S3 in the supplemental material).

Cloning and expression of recombinant proteins. The coding region of the large subunit was amplified by PCR using 5′-ATATATGGATCCG ATGGCGAATAATCATTACGACGCGA-3′ (forward primer; underlining indicates a restriction site) and 5′-ATATATGTCGACTTACAGATTT CCCTTCTTGAGCTCT-3′ (reverse primer). For the small subunit, primers 5′-ATATATCATATGCTGGATAAAGCCGCTGCGGCAAGG C-3′ (forward) and 5′-ATATATCTCGAGTCAGGCTGTGCCCCAAGC GGGCGTA-3′ (reverse) were used to amplify its coding gene. The PCR product for the large subunit was digested with BamHI and SalI, and the PCR product for the small subunit was digested with NdeI and XhoI. The two digested PCR products were cloned into multiple-cloning sites of the isopropyl-β-D-thiogalactopyranoside (IPTG)-inducible expression vector pETDuet-1 (EMD Bioscience, Darmstadt, Germany), which carries resistance to ampicillin. Additionally, the large subunit gene was cloned alone in pET28b. The large subunit gene was amplified by PCR for cloning in pET28b using 5′-ATATATCCATGGCGAATAATCATTACG ACGCGA-3′ (forward) and 5′-ATATATGTCGACTTACAGATTTCCCT TCTTGAGCTCT-3′ (reverse). Recombinant pET28b carrying the large subunit gene was introduced into *Escherichia coli* BW25113(DE3) which had already been transformed with the pBAD:groESL plasmid (donated from Sun-Gu Lee, Pusan National University) (24). Transformants of *E. coli* BW25113(DE3) were grown in LB broth containing 50 μg/ml of kanamycin, 100 μg/ml of ampicillin, and 1 mM L-arabinose from the beginning of the culture. The pETDuet-1 plasmid carrying the large- and small-subunit genes was introduced into *E. coli* Rosetta-gami 2(DE3, pLysS) (EMD Bioscience, Darmstadt, Germany), and the transformant was grown in LB broth containing 100 μg/ml of ampicillin at 37°C. For overexpression of proteins, IPTG was added to a final concentration of 0.5 mM for transformants of both *E. coli* BW25113 and *E. coli* Rosetta-gami 2 when the optical density at 600 nm (OD_{600}) reached 0.4 to 0.6. Cells were further incubated at 20°C for 12 h. The cells were harvested by centrifugation at 7,000 × *g* for 15 min at 4°C. The cell pellets were washed with PBS and resuspended in 5 ml of 50 mM Tris-HCl buffer (pH 7.4) containing 1 mM PMSF and 1 mM DTT. The crude extract was obtained by ultrasonic disruption, and cell debris was removed by centrifugation at 14,000 × *g* for 30 min at 4°C. The expressed large subunit was purified from the crude extract by Ni-nitrilotriacetic acid (NTA) affinity purification (Qiagen Korea, Seoul, Republic of Korea).

Analysis of the deglycosylation mechanism. The first reaction with the purified recombinant enzyme was performed in 1 ml of 50 mM sodium phosphate buffer (pH 6.5) containing 250 μM CK at 55°C for 90 min. The reaction mixture was extracted with 1 ml ethyl acetate, and the extracted sample was evaporated using a vacuum concentrator. Dried samples were dissolved in ethanol. Oxidized CK in ethanol was used as a substrate for the second reaction. The second reaction was performed in 1 ml of 50 mM sodium phosphate buffer (pH 8.0) containing oxidized CK for 12 h. Reactions were performed with and without purified enzyme, respectively. The second-reaction samples were extracted and dried by the method used for the first reaction. After reaction termination by addition of 1 ml of ethyl acetate, the reaction mixture was analyzed using HPLC.

Characterization of the recombinant enzyme. To determine the optimum reaction pH, an initial enzyme reaction rate was measured by analyzing the amount of oxidized CK in buffers with various pHs: pH 3.5 to 5.5 with 50 mM citrate buffer, pH 5.5 to 8.5 with 50 mM sodium phosphate buffer, and pH 8.5 to 10.5 with 50 mM borate buffer. For the determination of metal ion effects, divalent metal ions were added as chloride salts at 10 mM in the reaction mixture (Ca^{2+}, Mn^{2+}, Mg^{2+}, Fe^{2+}, Ni^{2+}, Co^{2+}, and Zn^{2+}). The optimum temperature was investigated by reactions at various temperatures ranging from 20°C to 65°C. Substrate specificity was investigated using various ginsenosides and glycosides. Kinetic constants were obtained from the oxidation reactions performed by varying the concentration of CK.

To identify flavin adenine dinucleotide (FAD) in the enzyme, the purified glycoside oxidoreductase was denatured by boiling for 10 min to release bound FAD. After the denatured protein was removed by centrifugation at 11,000 × *g*, light absorbance of the supernatant was measured at 450 nm using a UV-visible spectrometer (Hewlett-Packard 8453; Agilent Technologies, Foster City, CA). The extinction coefficient of FAD at 450 nm (11,300 M^{-1} cm^{-1}) (25) was used to determine the concentration of FAD in solution.

Nucleotide sequence accession numbers. The sequences of the large and small subunits of the enzyme identified in this study have been submitted to GenBank and given accession numbers JN683624 and JN683625, respectively.

RESULTS AND DISCUSSION

Screening and identification of the microorganism and the enzyme responsible for deglycosylation of CK. After several rounds of enrichment culture, a strain with CK deglycosylation activity was found. The whole-cell reaction using the screened microorganism yielded mass peaks of an Na^+ adduct of PPD(S) at *m/z* 483.547 Da and of a K^+ adduct of PPD(S) at *m/z* 499.500 Da, which were distinctly different peaks from the ones found in nonactive cells (Fig. 2). 16S rRNA sequencing of the screened microorganism showed 99% identity with the partial 16S rRNA gene of *Rhizobium* sp. strain R-31762 (99.2% identity [1,073/1,081]). Therefore, this microorganism was named *Rhizobium* sp. strain GIN611. The enzyme from *Rhizobium* sp. GIN611 cells, purified using fast protein liquid chromatography (FPLC), showed the same deglycosylation activity for CK. The final active fraction showed two major bands at about 65 kDa and 20 kDa by 12% SDS-PAGE (see Fig. S1 in the supplemental material), whereas the same sample showed a single peak at an estimated size of 85 kDa in

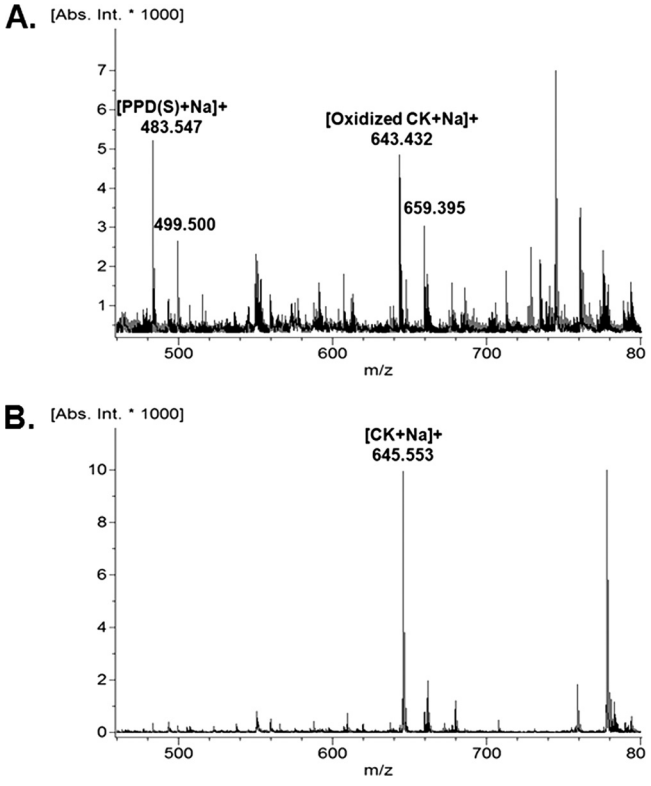

FIG 2 Analysis of CK deglycosylation. (A) MALDI-TOF spectrum of the active microorganism. The peaks at m/z = 483.547 and 643.432 are the sodium ion adduct $[PPD(S)+Na]^+$ and $[CK-2H+Na]^+$ peaks, respectively. (B) Spectrum of the reaction mixture with nonactive microorganism. The peak at 645.553 is the sodium ion adduct peak of substrate CK. Abs. Int., absorption intensity.

gel permeation chromatography. The single band in the native PAGE analysis was split into two protein bands on SDS-PAGE (see Fig. S2 in the supplemental material), suggesting that it is a complex of two proteins. The two subunits were inseparable when heat treated at 95°C for 10 min without DTT and were separable only when treated with DTT at a final concentration of 100 mM, suggesting that the two subunits are covalently linked with disulfide bonds. However, the formation of disulfide bonds in the cytoplasm is an exceedingly rare event (4). Therefore, although it is not clear whether the disulfide bond is formed *in vivo* or during the purification step, the existence of the disulfide bond between the two proteins is confirmed by the experiment. Formation of a disulfide bond between the two proteins indicates that the large subunit and small subunit interact and that two cysteine residues exist at the interface.

To clone the enzyme, the N-terminal sequences of the large subunit and small subunit were identified as ANNHYDAIVV and LDKAA, respectively. Their internal peptide sequences were obtained using mass spectrometry (see Table S1 in the supplemental material). A BLAST search using the N-terminal peptide sequence (ANNHYDAIVV) of the large subunit predicted that it is 100% identical to the N-terminal fragment of glucose-methanol-choline (GMC) oxidoreductase (gi 4174446) from *Pseudoalteromonas atlantica* T6c and that one of the internal peptide sequences (AADFAVSELKK) is 90% identical to the sequence of the C-terminal region of oxidoreductase (gi 8724182) from *Sphingobacterium spiritivorum* ATCC 33861. However, a BLAST search with the N terminus and two internal peptide sequences of the small subunit did not indicate any protein sequences with significant identity.

Identification of coding sequences and protein function. The degenerate primers listed in Table S1 in the supplemental material were used for PCR to find the coding sequence of the large subunit of the purified enzyme. When the forward and reverse degenerate primers based on the N-terminal peptide (ANNHYDAIVV) and the internal peptide (AADFAVSELKK), respectively, were used to perform PCR using genomic DNA of *Rhizobium* sp. GIN611, a 1,674-bp DNA fragment was obtained. The protein sequence deduced from the PCR product matched with 13 peptide sequences obtained from *de novo* sequencing by linear trap quadrupole-tandem MS (LTQ-MS) (see Fig. S3 in the supplemental material). However, the whole fragment lacked information about the C-terminal region of the large subunit, including a stop codon of the transcript. A self-ligated genomic DNA library of *Rhizobium* sp. GIN611 was generated using HindIII, and the library was subjected to inverse PCR to amplify the outward gene sequence of the obtained partial sequence (see Materials and Methods). A 1-kb PCR product was obtained and sequenced. The remaining C-terminal DNA sequence of the large subunit, including a TAA stop codon, was identified. Interestingly, the sequence from the 1-kb PCR product, including the C terminus of the large-subunit protein, also contained the sequence of the small-subunit protein. A comparison of the deduced protein sequences of the small-subunit protein and the N terminus and two other internal sequences obtained from *de novo* sequencing of the small-subunit protein showed good agreement (see Fig. S3 and Table S1 in the supplemental material). The analysis revealed that the two subunits of the purified deglycosylating enzyme were encoded by an operon (2,243 bp) in *Rhizobium* sp. GIN611. The full DNA and amino acid sequences are shown in Fig. S3 in the supplemental material. The large-subunit protein consisted of 561 amino acid residues (1,686 bp) with a theoretical pI of 5.86 and a molecular mass of 63,379 Da. The small-subunit protein consisted of 185 amino acid residues (558 bp) with a theoretical pI of 5.17 and a molecular mass of 20,368 Da. The start codon (ATG) of the small subunit overlapped with the last nucleotide of the stop codon (TAA) of the large subunit.

The complete amino acid sequences of the large- and small-subunit proteins deduced from the DNA sequences are shown in Fig. S3 in the supplemental material. The large-subunit protein of *Rhizobium* sp. GIN611 showed the highest identity (93%) to oxidoreductase (gi 1136251) from *Agrobacterium tumefaciens* strain C58. A glucose-methanol-choline (GMC) oxidoreductase (gi 6495394) from *Stenotrophomonas maltophilia* K279a had the next highest identity (75%). The small subunit showed the highest identity (72%) to a hypothetical protein (gi 1136252) from *Agrobacterium tumefaciens* strain C58 and the second highest identity (44%) to a putative transmembrane protein (gi 6395363) from *Stenotrophomonas maltophilia* K279a. According to analysis with the Conserved Domain Database (CDD) (27) in the NCBI sequence analysis tool box, the large-subunit protein is predicted to have a FAD binding motif (i.e., GSGISG) in its N-terminal region, which is exactly matched to a known FAD binding motif, GXGXXG (36). In conclusion, the large-subunit protein appears to be a putative FAD-dependent protein.

Overexpression and characterization of the two subunit proteins in *E. coli*. To determine which subunit has the deglycosyla-

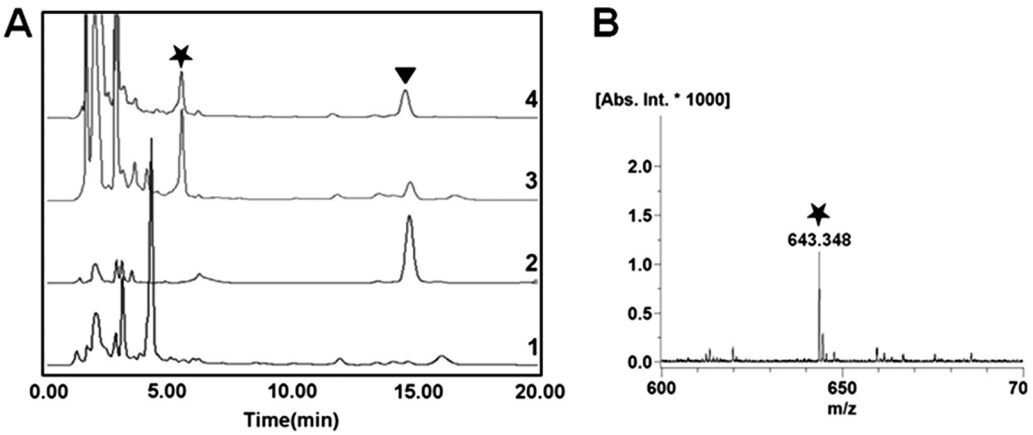

FIG 3 HPLC analysis of glycoside oxidoreductase with purified recombinant large subunit. (A) Line 1, authentic CK (RT, 4.7 min); line 2, authentic PPD(S) (RT, 15 min); line 3, 3-h reaction sample; line 4, 12-h reaction sample. (B) MALDI-MS spectrum of the 5.5-min-RT peak in HPLC. The star and inverted triangle indicate the oxidized CK and PPD(S), respectively.

tion activity, each subunit was cloned and overexpressed separately in *E. coli* Rosetta-gami 2(DE3, pLysS). The small subunit was overexpressed in soluble form, but it did not show any deglycosylation activity for CK. The large-subunit protein could be overexpressed, but only as an insoluble form in spite of the use of the GroEL/GroES chaperone system (see Fig. S4B in the supplemental material). It was later found that the large-subunit protein can be overexpressed in soluble form, but only when the small subunit is coexpressed. However, a purified recombinant large-subunit protein alone (see Fig. S4D in the supplemental material) exhibits the same deglycosylation activity for CK. When the two proteins were coexpressed using one vector in the same *E. coli* host strain, the His_6-tagged large-subunit protein purified with an Ni-agarose column did not appear to be accompanied by the small-subunit protein, suggesting that the recombinant large-subunit protein from *E. coli* does not covalently bind to the recombinant

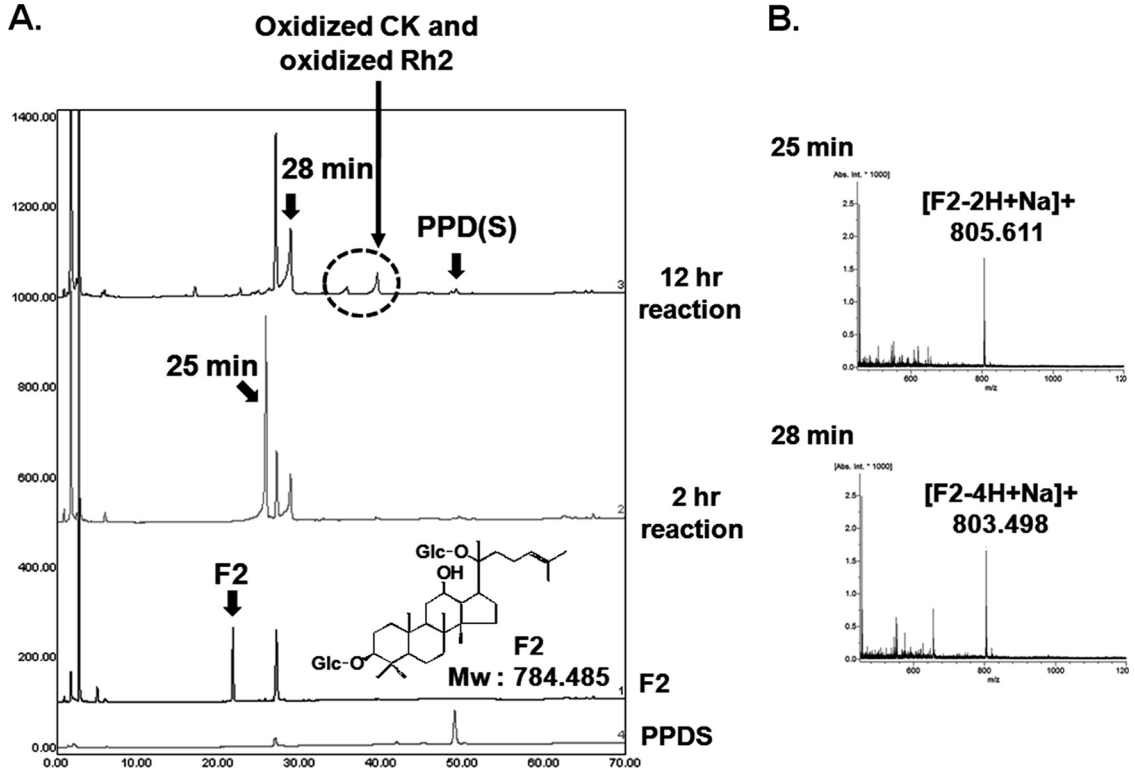

FIG 4 (A) HPLC analysis of F2 reaction. The dashed circle indicates the peaks of oxidized CK and oxidized Rh2. (B) MALDI-MS result for peaks at 25-min and 28-min RTs. The sodium ion adduct $[F2\text{-}2H+Na]^+$ and $[F2\text{-}4H+Na]^+$ peaks at m/z = 805.611 and 803.498 at 25-min and 28-min RTs, respectively, indicate the oxidation of one glucose moiety in F2 and subsequent oxidation of the two glucose moieties in F2, respectively. The molecular mass of F2 is 784.48 (that of $[F2+Na]^+$ is 807.487).

TABLE 1 Substrate specificities of glycoside oxidoreductase

Substrate	Intermediate(s)	Final product
Rb1	Oxidized intermediate of ginsenosides and deglycosylated ginsenosides	PPD(S)
Rb2	Oxidized intermediate of ginsenosides and deglycosylated ginsenosides	Compound Y
Rb3	Oxidized intermediate of ginsenosides and deglycosylated ginsenosides	PPD(S)
Rc	Oxidized intermediate of ginsenosides and deglycosylated ginsenosides	Mc
F2	Oxidized F1, oxidized Rh2, oxidized CK	PPD(S)
Rh2	Oxidized Rh2	PPD(S)
CK	Oxidized CK	PPD(S)
Re	Oxidized Re	Rg2
F1	Oxidized F1	PPT(S)
Camelliaside A	Oxidized camelliaside A	6-*O*-Rha-kampferol
Camelliaside B	Oxidized camelliaside B	6-*O*-Rha-kampferol
Icariin	Oxidized icariin	Icariside
Daidzin	Oxidized daidzin	Daidzein

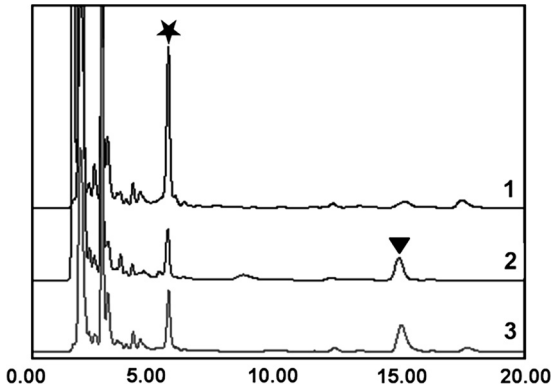

FIG 5 Reaction results using oxidized CK. Line 1, reaction without the oxidoreductase enzyme (0-h reaction, control); line 2, reaction with the enzyme for 12 h; line 3, reaction without the enzyme for 12 h. The star and inverted triangle indicate oxidized CK and PPD(S), respectively.

small subunit (see Fig. S2 and S4C and D in the supplemental material). This result indicates that the small-subunit protein is not essential for the deglycosylation activity but is required to make the large-subunit protein soluble and active.

The His_6-tagged recombinant large-subunit protein showed a distinctive yellow color like that of the purified enzyme complex from *Rhizobium* sp. GIN611. After enough of the recombinant large-subunit protein was prepared, the presence of FAD in the protein was analyzed by boiling and UV spectrometry. After boiling of the protein solution and subsequent removal of aggregate debris by centrifugation, the resulting supernatant yielded a yellow color, suggesting that the FAD cofactor was not covalently bound to the enzyme. Maximum absorption of the extracted cofactor was obtained at 375 to 445 nm, corresponding to the characteristic absorption peaks of FAD (see Fig. S7 in the supplemental material). The FAD-oxidoreductase stoichiometry was determined to be 1:1.9, suggesting that the oxidoreductase contained 1 molecule of FAD per monomer oxidoreductase (considering that the sample contained some contaminating proteins).

Analysis of the deglycosylation reaction mechanism. The identification of the purified protein as an oxidoreductase enzyme with a FAD binding domain rather than a glucosidase was very intriguing and unexpected. One interpretation of this result is a possible misannotation of a putative glucosidase, and the other possibility is that an unknown oxidoreductase is involved in this deglycosylation of ginsenoside. The reaction mixture was analyzed by HPLC to find any unexpected reaction intermediates, and one such peak was detected at a retention time (RT) of 5.5 min, as shown in Fig. 3A. The resulting hydrolyzed PPD(S) was eluted at 15 min under the same conditions. The sample from the 5.5-min peak was collected and analyzed by MALDI-TOF. It had a molecular mass of 643.348 Da, which was 2 Da smaller than the molecular mass of the substrate, CK (Fig. 3B). The same molecular mass was also found from the reaction mixture with the whole-cell pellet (Fig. 2), suggesting that an unknown function of the purified deglycosylating enzyme always led to the loss of 2 Da from the molecular mass of CK in the reaction mixture. In addition, the time course HPLC analysis of the reaction mixture showed that PPD(S) production was followed by the initial accumulation of the unknown peak with the 2-Da-lower molecular mass (Fig. 3A). One hypothesis drawn from this result was that the oxidation of CK is not a side reaction product catalyzed by this enzyme but is a main product with a loss of two protons from the glucose moiety in CK. After this oxidation, a subsequent deglycosylation reaction occurs. To confirm this hypothesis, the other substrate, F2, was subjected to the same reaction using the same purified recombinant enzyme. MALDI-TOF analysis showed that the purified recombinant enzyme had the same deglycosylating activity for F2, resulting in PPD(S) (see Fig. S5 in the supplemental material). In Fig. 4, the two peaks with RTs of 25 min and 28 min had molecular masses of 805.611 Da and 803.498 Da, corresponding to $[F2\text{-}2H+Na]^+$ and $[F2\text{-}4H+Na]^+$, respectively, suggesting that, like in the case of the CK reaction, the losses of two protons would take place at two different glucose positions in F2. Again, no other products indicating any mass losses from the product PPD(S) were detected. These results led us to the conclusion that the oxidoreductase primarily catalyzes oxidation of glucose moieties of CK and F2 and the subsequent deglycosylation reaction takes place in the oxidized intermediates by an unknown mechanism. Time profile analyses of the reaction mixtures used for Fig. 3 and 4 also showed that the nondeglycosylated oxidized CK and F2 accumulated at the beginning and decreased with time. The final product, PPD(S), gradually increased in both cases, suggesting that the oxidation reaction was much faster than the deglycosylation reaction. To investigate the deglycosylation reaction mechanism, oxidized CK prepared by extraction from the first reaction mixture was used for the second reaction. As shown in Fig. 5, after the 12-h reaction, the deglycosylation reaction took place even

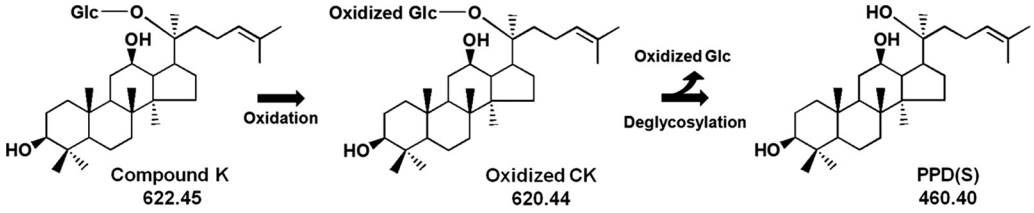

FIG 6 Proposed reaction pathway for deglycosylation of CK by glycoside oxidoreductase.

without the enzyme, indicating that the deglycosylation reaction, i.e., the production of PPD(S) from the oxidized form of CK, is spontaneous.

Characterization of the FAD-dependent glycoside oxidoreductase from *Rhizobium* sp. GIN611. The recombinant FAD-dependent glycoside oxidoreductase showed the highest activity at pH 6.5 and 55°C. Addition of Ca^{2+} ion resulted in slightly higher enzyme activity than that in the absence of the metal ion (see Fig. S6 in the supplemental material). The optimized conditions were used for further characterization of the FAD-dependent glycoside oxidoreductase. It had broad specificities toward glycosides having various aglycons, including isoflavones such as daidzin and flavonoids such as camelliaside A, camelliaside B, and icariin. It also showed broad specificities toward sugar moieties such as glucose, galactose, and xylose (see Fig. S8 in the supplemental material). When analyzed by MALDI-TOF, all the reaction mixtures with different substrates were found to contain corresponding oxidized intermediates and deglycosylated products (Table 1; see Table S2 in the supplemental material), suggesting that this oxidoreductase had broad specificities toward glycones and aglycons. The enzyme reaction rate calculated by measuring the concentrations of oxidized CK was rather low, with a k_{cat} of 2.71 s^{-1}, a K_m of 0.11 mM, and a k_{cat}/K_m ratio of 2.4×10^4 M^{-1} s^{-1}. The yield of the products was over 88% after 30 min at 2 mM CK, and CK converted oxidized CK completely within 1 h. The oxidized CK was fully deglycosylated within 12 h.

Conclusion. In this paper, we report on a novel FAD-dependent glycoside oxidoreductase from *Rhizobium* sp. GIN611 as an interesting biocatalyst for the oxidation of ginsenoside, which results in deglycosylation. The CK deglycosylation enzyme shows its deglycosylating activity through the oxidation of the glucose moiety of ginsenosides, and the subsequent deglycosylation reaction occurs spontaneously on its own (Fig. 6). The reaction mechanism appears to be by double bond generation in the glucose moiety of CK as deduced from the molecular mass analysis using mass spectrometry. In addition, the glycoside oxidoreductase is active toward other glycone units bound to ginsenoside Rb3 (-Xyl), camelliaside A (-Gal), and camelliaside B (-Xyl), suggesting that its deglycosylation activity is not glycone specific like that of many other glycosidases. This deglycosylation mechanism is quite different from that of common glycosidases. In a BLAST search, the glycoside oxidoreductase showed high sequence identities with members of the FAD-dependent glucose-methanol-choline oxidoreductase family. The glycoside oxidoreductase consists of two subunits, one large (63.5 kDa) and one small (17.5 kDa). The small-subunit protein was found to help the soluble expression of the glycoside oxidase. From these results, it could be verified that the oxidoreductase is responsible for the CK deglycosylation reaction, rather than there having been a misannotation of a glucosidase in the enzyme database.

It is well known that the deglycosylation of glycosides is mediated by the traditional β-glucosidase mechanism (30). In this research, we demonstrated that the deglycosylation of ginsenoside can occur through the oxidation of glucose by oxidoreductase and subsequent spontaneous deglycosylation. Furthermore, because the glycoside oxidoreductase of *Rhizobium* sp. GIN611 has broad substrate specificity for various kinds of aglycons and glycones, this enzyme appears to be quite a promising biocatalyst for preparation of aglycons from ginsenosides as well as various glycoconjugate natural compounds.

ACKNOWLEDGMENTS

This work was supported by the Seoul R&BD Program (KU080657M0209721) and a National Research Foundation of Korea (NRF) grant funded by the Korean government (MEST) (20090083035) and by the World Class University (WCU) program through the Korea Science and Engineering Foundation funded by the Ministry of Education, Science and Technology (R32-2008-000-10213-0).

REFERENCES

1. **Andreea Neculai M, Ivanov D, Bernards MA.** 2009. Partial purification and characterization of three ginsenoside-metabolizing beta-glucosidases from Pythium irregulare. Phytochemistry **70**:1948–1957.
2. **Bae EA, Han MJ, Choo MK, Park SY, Kim DH.** 2002. Metabolism of 20(S)- and 20(R)-ginsenoside Rg3 by human intestinal bacteria and its relation to in vitro biological activities. Biol. Pharm. Bull. **25**:58–63.
3. **Bae EA, Shin JE, Kim DH.** 2005. Metabolism of ginsenoside Re by human intestinal microflora and its estrogenic effect. Biol. Pharm. Bull. **28**: 1903–1908.
4. **Bessette PH, Aslund F, Beckwith J, Georgiou G.** 1999. Efficient folding of proteins with multiple disulfide bonds in the Escherichia coli cytoplasm. Proc. Natl. Acad. Sci. U. S. A. **96**:13703–13708.
5. **Cameron RG, Manthey JA, Baker RA, Grohmann K.** 2001. Purification and characterization of a beta-glucosidase from Citrus sinensis var. Valencia fruit tissue. J. Agric. Food Chem. **49**:4457–4462.
6. **Chen CF, Chiou WF, Zhang JT.** 2008. Comparison of the pharmacological effects of Panax ginseng and Panax quinquefolium. Acta Pharmacol. Sin. **29**:1103–1108.
7. **Chen GT, et al.** 2008. Microbial transformation of ginsenoside Rb(1) by Acremonium strictum. Appl. Microbiol. Biotechnol. **77**:1345–1350.
8. **Cheng LQ, Na JR, Bang MH, Kim MK, Yang DC.** 2008. Conversion of major ginsenoside Rb1 to 20(S)-ginsenoside Rg3 by Microbacterium sp. GS514. Phytochemistry **69**:218–224.
9. **Chi H, Kim DH, Ji GE.** 2005. Transformation of ginsenosides Rb2 and Rc from Panax ginseng by food microorganisms. Biol. Pharm. Bull. **28**: 2102–2105.
10. **Choi K, Choi C.** 2009. Proapoptotic ginsenosides compound K and Rh enhance Fas-induced cell death of human astrocytoma cells through distinct apoptotic signaling pathways. Cancer Res. Treat. **41**:36–44.
11. **Gatlin CL, Kleemann GR, Hays LG, Link AJ, Yates JR III.** 1998. Protein identification at the low femtomole level from silver-stained gels using a new fritless electrospray interface for liquid chromatography-microspray and nanospray mass spectrometry. Anal. Biochem. **263**:93–101.
12. **Han BH, et al.** 1982. Degradation of ginseng saponins under mild acidic conditions. Planta Med. **44**:146–149.
13. **Han Y, et al.** 2007. Transformation of bioactive compounds by Fusarium

sacchari fungus isolated from the soil-cultivated ginseng. J. Agric. Food Chem. **55**:9373–9379.
14. **Hasegawa H.** 2004. Proof of the mysterious efficacy of ginseng: basic and clinical trials: metabolic activation of ginsenoside: deglycosylation by intestinal bacteria and esterification with fatty acid. J. Pharmacol. Sci. **95**: 153–157.
15. **Hasegawa H, Sung JH, Benno Y.** 1997. Role of human intestinal Prevotella oris in hydrolyzing ginseng saponins. Planta Med. **63**:436–440.
16. **Hasegawa H, Sung JH, Matsumiya S, Uchiyama M.** 1996. Main ginseng saponin metabolites formed by intestinal bacteria. Planta Med. **62**: 453–457.
17. **Kim DH, et al.** 2003. Inhibition of intracerebroventricular injection stress-induced plasma corticosterone levels by intracerebroventricularly administered compound K, a ginseng saponin metabolite, in mice. Biol. Pharm. Bull. **26**:1035–1038.
18. **Kim DY, et al.** 2009. Compound K induces apoptosis via CAMK-IV/AMPK pathways in HT-29 colon cancer cells. J. Agric. Food Chem. **57**: 10573–10578.
19. **Kim MK, Lee JW, Lee KY, Yang DC.** 2005. Microbial conversion of major ginsenoside rb(1) to pharmaceutically active minor ginsenoside rd. J. Microbiol. **43**:456–462.
20. **Kim S, et al.** 2004. Compound K induces expression of hyaluronan synthase 2 gene in transformed human keratinocytes and increases hyaluronan in hairless mouse skin. Biochem. Biophys. Res. Commun. **316**: 348–355.
21. **Kitagawa S, Takahashi T, Nabekura T, Tachikawa E, Hasegawa H.** 2007. Inhibitory effects of ginsenosides and their hydrolyzed metabolites on daunorubicin transport in KB-C2 cells. Biol. Pharm. Bull. **30**:1979–1981.
22. **Ko SR, Choi KJ, Suzuki K, Suzuki Y.** 2003. Enzymatic preparation of ginsenosides Rg2, Rh1, and F1. Chem. Pharm. Bull. (Tokyo) **51**:404–408.
23. **Ko SR, Suzuki Y, Suzuki K, Choi KJ, Cho BG.** 2007. Marked production of ginsenosides Rd, F2, Rg3, and compound K by enzymatic method. Chem. Pharm. Bull. (Tokyo) **55**:1522–1527.
24. **Lee JH, et al.** 2008. Improving the growth rate of Escherichia coli DH5alpha at low temperature through engineering of GroEL/S chaperone system. Biotechnol. Bioeng. **99**:515–520.
25. **Lewis JA, Escalante-Semerena JC.** 2006. The FAD-dependent tricarballylate dehydrogenase (TcuA) enzyme of Salmonella enterica converts tricarballylate into cis-aconitate. J. Bacteriol. **188**:5479–5486.
26. **Liu TG, et al.** 2009. Inhibitory effect of ginsenoside Rg3 combined with gemcitabine on angiogenesis and growth of lung cancer in mice. BMC Cancer **9**:250.
27. **Marchler-Bauer A, et al.** 2009. CDD: specific functional annotation with the Conserved Domain Database. Nucleic Acids Res. **37**:D205–D210.
28. **Ota T, Maeda M, Odashima S.** 1991. Mechanism of action of ginsenoside Rh2: uptake and metabolism of ginsenoside Rh2 by cultured B16 melanoma cells. J. Pharm. Sci. **80**:1141–1146.
29. **Park SY, Bae EA, Sung JH, Lee SK, Kim DH.** 2001. Purification and characterization of ginsenoside Rb1-metabolizing beta-glucosidase from Fusobacterium K-60, a human intestinal anaerobic bacterium. Biosci. Biotechnol. Biochem. **65**:1163–1169.
30. **Rye CS, Withers SG.** 2000. Glycosidase mechanisms. Curr. Opin. Chem. Biol. **4**:573–580.
31. **Shibata S.** 2001. Chemistry and cancer preventing activities of ginseng saponins and some related triterpenoid compounds. J. Korean Med. Sci. **16**(Suppl):S28–S37.
32. **Shin HY, Park SY, Sung JH, Kim DH.** 2003. Purification and characterization of alpha-L-arabinopyranosidase and alpha-L-arabinofuranosidase from Bifidobacterium breve K-110, a human intestinal anaerobic bacterium metabolizing ginsenoside Rb2 and Rc. Appl. Environ. Microbiol. **69**:7116–7123.
33. **Son JW, Kim HJ, Oh DK.** 2008. Ginsenoside Rd production from the major ginsenoside Rb(1) by beta-glucosidase from Thermus caldophilus. Biotechnol. Lett. **30**:713–716.
34. **Tawab MA, Bahr U, Karas M, Wurglics M, Schubert-Zsilavecz M.** 2003. Degradation of ginsenosides in humans after oral administration. Drug Metab. Dispos. **31**:1065–1071.
35. **Wang W, et al.** 2007. In vitro anti-cancer activity and structure-activity relationships of natural products isolated from fruits of Panax ginseng. Cancer Chemother. Pharmacol. **59**:589–601.
36. **Wierenga RK, Terpstra P, Hol WG.** 1986. Prediction of the occurrence of the ADP-binding beta alpha beta-fold in proteins, using an amino acid sequence fingerprint. J. Mol. Biol. **187**:101–107.
37. **Yan Q, et al.** 2008. Purification and properties of a novel beta-glucosidase, hydrolyzing ginsenoside Rb1 to CK, from Paecilomyces bainier. J. Microbiol. Biotechnol. **18**:1081–1089.
38. **Ye L, et al.** 2011. Biotransformation of ginsenoside Rb1 to ginsenoside Rd by highly substrate-tolerant Paecilomyces bainier 229-7. Bioresour. Technol. **101**:7872–7876.
39. **Yim JS, et al.** 2004. Metabolic activities of ginsenoside Rb1, baicalin, glycyrrhizin and geniposide to their bioactive compounds by human intestinal microflora. Biol. Pharm. Bull. **27**:1580–1583.
40. **Yu H, et al.** 2007. Purification and characterization of new special ginsenosidase hydrolyzing multi-glycisides of protopanaxadiol ginsenosides, ginsenosidase type I. Chem. Pharm. Bull. (Tokyo) **55**:231–235.
41. **Zhang C, Yu H, Bao Y, An L, Jin F.** 2001. Purification and characterization of ginsenoside-beta-glucosidase from ginseng. Chem. Pharm. Bull. (Tokyo) **49**:795–798.